Journal of Materials and Metallurgical Engineering
Volume 2, Issue 2, August 2012, Pages

Processing and Characterization of Ni_2MnSn FSMA

Ajit Behera**, S. C. Mishra
Department of Metallurgical & Materials Engineering, National Institute of Technology, Rourkela-769008, Odisha, India

ABSTRACT

Among Ferromagnetic Shape Memory alloys (FSMAs), Ni2MnSn Heusler alloys owing to occurrence of large magnetic field induced strain (> 10%) along with other interesting properties like premartensitic transition, high transformation temperature, large magnetocaloric effect and low stress of twin variant rearrangement. The prominent challenges facing the design and utilization of these specialized alloys are a limited range of operating temperatures, phase transformations that have high sensitivity to variations in composition, brittleness of the alloys, and changes in transformation temperatures. The functional behaviors of these alloys are as actuators, magneto-mechanical transducers, switching devices, etc. In the present study, the martensitic microstructures of Ni50Mn37.5Sn12.5 FSMAs are investigated by optical microscopy, X-ray diffraction, differential scanning calorimetry, and transmission electron microscopy. Among the most important martensites that exist in these alloys are the 5M tetragonal, 7M orthorhombic (modulated structures) and NM tetragonal (non-modulated structure), etc. Differential scanning calorimeter is used for determining the transformation temperatures under zero stress. Crystal structures of the samples are determined by X-ray diffraction patterns using Cu-Kα radiations. Transmission electron microscopy study of this alloy revealed the presence of two martensite phases, i.e., modulated and non-modulated phases.

Keywords: *FSMA, Ni_2MnSn, transformation temperature*

****Author for Correspondence*** Email: ajit.behera88@gmail.com

1. INTRODUCTION

Shape Memory Alloys (SMAs) exhibit Shape Memory Effect (SME) that can be driven not only by temperature and stress but also by magnetic field. The magnetic field-controlled SME has a rapid and efficient response, which makes FSMAs have more applications than conventional shape memory alloys [1]. Ni-Mn-Sn-based Heusler alloys are considered as one of the new Ga-free FSMAs which can offer an alternative to the more established Ni-Mn-Ga alloy system. The compound Ni_2MnSn (parent phase) has the cubic L_21-structure. In this structure, the Ni ions occupy the site of the cube corners (8c-site), and Mn and Sn ions are in the alternate body centers of the successive cubes (4a- and 4c-sites, respectively). Few investigations are made on the structural transformation in the stoichiometric compound Ni_2MnSn. Suto et al. found that the Heusler FSMAs $Ni50Mn_{50-y}X_y$(X = In, Sn, and Sb) show the martensitic transformation (MT) from the L_21 structure to an orthorhombic (4O) structure in the ferromagnetic state [2]. The MT in these alloys is often accompanied by the abrupt changes of magnetization and resistance, which result in several interesting phenomena around MT, such as meta-magnetic SME, large magneto-resistance [3–5], and large magneto-caloric effect (MCE) [6–14]. So, the applications of Ni_2MnSn FSMAs are highly expected in actuator, sensor, and magnetic

refrigerator etc. In the case of Ni_2MnSn system, the austenitic phase has a cubic L_21 structure, whereas the structure of the martensitic phase can be 10M, 14M, L_10, 4O depending on composition [15–17]. The first order martensitic transformation in Heusler-based alloys, influenced by the disorder, developed a region of metastability with austenite and the martensite coexisting together [18–20]. The transformation temperatures of FSMAs strongly depend on the composition and their values spread in a very wide range [21–22]. Crystallographic reversibility in SMAs is achieved by particular conditions of lattice parameters of the austenite and the martensite as well as the existence of many mobile twins [23].

2. EXPERIMENTAL PROCEDURE

A ternary intermetallic polycrystalline compound $Ni_{50}Mn_{37.5}Sn_{12.5}$ FSMAs Heusler alloy was prepared by non-consumable arc-melting. The commercial purities of used Ni, Mn, Sn are 99.95%, 99.9% and 99.99% respectively. The melting was carried out under high-purity atmosphere (99.996%). For the preparation of alloy ingot, the melting chamber was evacuated to a pressure of 10^{-5} torr and then was purged with pure argon. The process of evacuation and purging was repeated up to three times. The melting was carried out in an argon atmosphere and at a chamber pressure of nearly 10^{-5} torr. For complete homogenization of the alloy, the entire melting process was repeated several times. Then the alloy was cast into a rod form shown in Figure 1. This composition transforms martensite at room temperature (Ms = 67 ° C) with martensitic Curie temperature, Tc close to room temperature (14 ° C). The ingot was sealed in a quartz ampoule filled with helium gas and solutionized at 1000°C for 24 hr for homogenization. The martensitic transformation and phase in these alloys successfully characterized by using optical microscopy, X-ray diffraction, differential scanning calorimetry and transmission electron microscopy.

Fig. 1: *Prepared Sample of $Ni_{50}Mn_{37.5}Sn_{12.5}$ Heusler FSMA.*

3. RESULTS AND DISCUSSION

3.1. Optical Microscopy

In Figure 2 (a), different martensitic layers are present with different orientation in each grain of the sample at room temperature. The phase transformation results from a cooperative and collective motion of atoms on distances smaller than the lattice parameters. The absence of diffusion makes the martensitic phase transformation almost instantaneous. Figure 2 (b) shows magnified image of martensitic layer with 20 × magnification, present at Ni_2MnSn sample. The crystal lattice of the martensitic phase has lower symmetry

than that of the parent austenitic phase so that several variants of martensite can be formed from the same parent phase crystal. Magnetic shape memory effect in these materials involves the movement of twin boundaries which results in the growth of one of the twin variants at the expense of the other in response to an applied magnetic field below the martensitic transformation temperature [24].

The microstructure of Ni_2MnSn sample taken from optical microscope is given below:

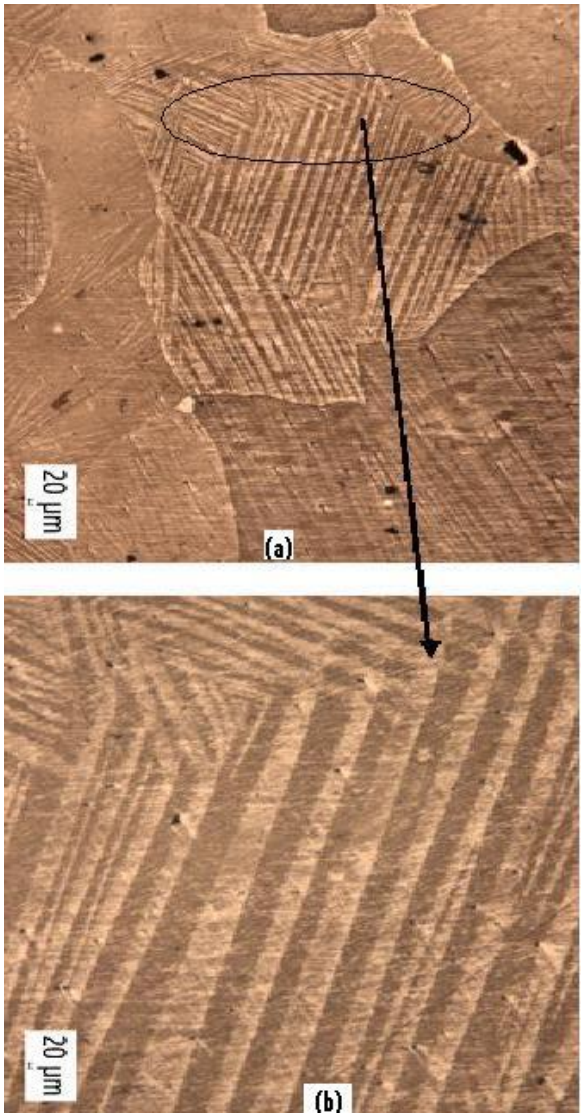

Fig. 2: *(a) A number of martensitic layers present in $Ni_{50}Mn_{37.5}Sn_{12.5}$, (b) enlarged martensitic layer at 20 × magnification.*

3.2. X-Ray Diffraction

A thin slice was cut from $Ni_{50}Mn_{37.5}Sn_{12.5}$ FSMA rod with a slow speed diamond wafering saw, polished, and cleaned with acetone with the aid of an ultrasonic cleaner. The slice was mounted on an XRD specimen holder and X-ray diffraction was obtained by using Cu-Kα radiation at room temperature. In Figure 3, in $Ni_{50}Mn_{37.5}Sn_{12.5}$ alloy, the peak reflections indexed as Ni (010), Ni (200), Mn (320), Mn (420), Mn (422) and Sn (411) confirm the existence of the highly ordered L_21 structure.

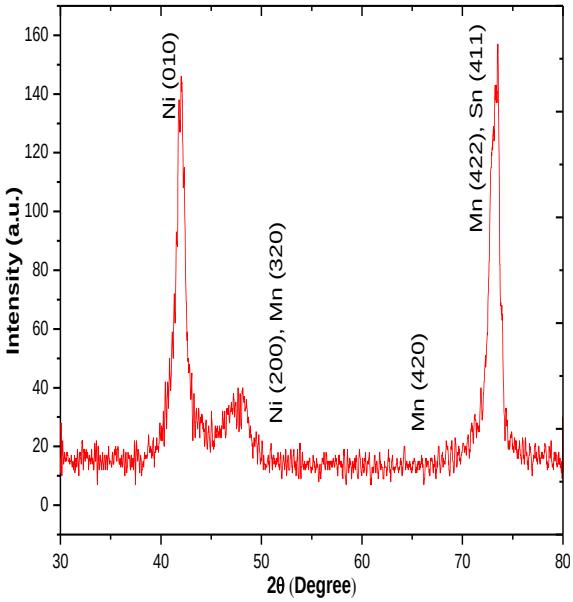

Fig. 3: *X-Ray Diffraction of $Ni_{50}Mn_{37.5}Sn_{12.5}$. The crystalline Structure Is Cubic L_21.*

3.3. Differential Scanning Calorimetry

Thermal analysis is useful to determine transformation temperatures in ferromagnetic alloys with structural transformations [25–29]. The alloy absorbs, or emits, heat over a small change in the specimen temperature, when there is a phase transformation occurring in the

material. In Figure 4, arrow 1 corresponds to forward martensitic transformation and arrow 2 corresponds to reverse martensitic transformation. Martensitic start temperature, martensitic finish temperature, austenitic start temperature and austenitic finish temperature are denoted as M_s, M_f, A_s, A_f respectively. In this test, the temperature was raised from −20 °C to 150 °C and lowered from 150 °C to −20 °C at a rate of 5 °C/min. M_s, M_f, A_s and A_f temperatures obtained are 53.56 °C, 40.24 °C, 64.70 °C, 78.95 °C respectively.

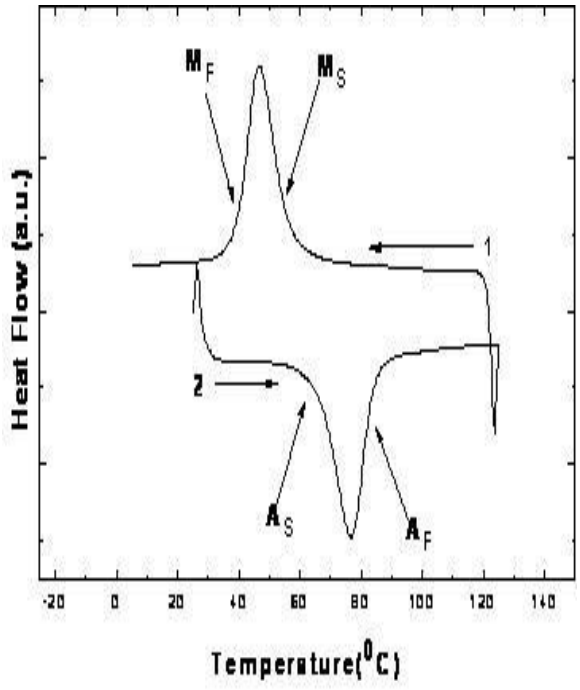

Fig.4: *Martensitic Transformations for Sample* $Ni_{50}Mn_{37.5}Sn_{12.5}$.

3.4. Transmission Electron Microscopy

Figure 5 (a) shows an internally-twinned tetragonal non-modulated-type and orthogonal modulated-type martensite and Figure 5 (b) reveals non-modulated zone which corresponds to twin diffraction pattern.

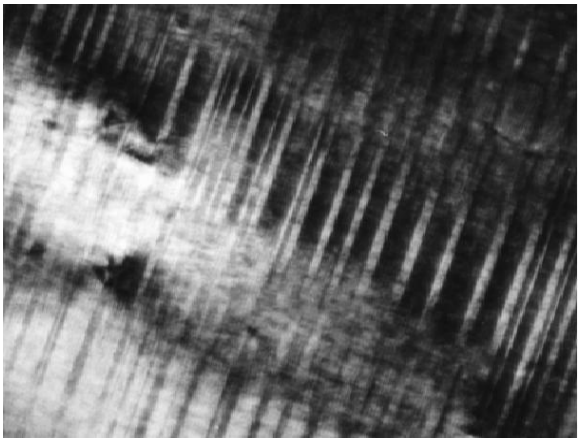

(a)

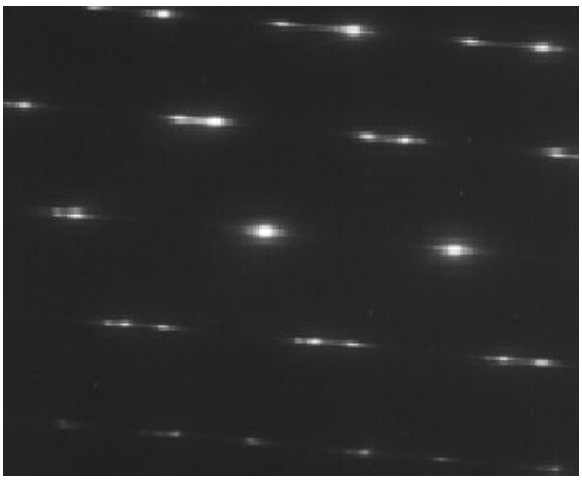

(b)

Fig. 5: *(a) The TEM Micrograph of* $Ni_{50}Mn_{37.5}Sn_{12.5}$ *(b) The SAD Pattern.*

4. CONCLUSIONS

The results indicate that several structural type (i.e., modulated/non-modulated) martensite can be formed by selecting the rate of cooling to obtain tailor-made structural morphology for captive use of such material.

ACKNOWLEDGEMENT

Authors acknowledge Materials Science Division BARC, Mumbai, as a part of the

work has been carried out there during summer training program.

REFERENCES

1. Z. D. Han et al. *Materials Science and Engineering B*. 2009. 157. 40–43.
2. Y. Suto et al. *Applied Physics Letters*. 2004. 85. 4358p. doi: 10.1063/1.1808879.
3. S. Y. Yu et al. *Applied Physics Letters*. 2006. 89. 162503. doi: 10.1063/1.2362581.
4. K. Koyama et al. *Applied Physics Letters*. 2006. 89. 182510. doi: 10.1063/1.2374868.
5. S. Y. Yu, L. Ma et al. *Applied Physics Letters*. 2007. 90. 242501. doi:10.1063/1.2748095.
6. P. A. Bhobe et al. *Applied Physics Letters*. 2007. 91. 242503. doi:10.1063/1.2823601.
7. Z. D. Han et al. *Applied Physics Letters*. 2007. 90. 042507. doi:10.1063/1.2435593.
8. T. Krenke et al. *Nature Material* 2005.4. 450. doi:10.1038/nmat1395.
9. T. Krenke et al. *Journal of Applied Physics*. 2007. 102. 033903. doi:10.1063/1.2761853.
10. S. Aksoy et al. *Applied Physics Letters*. 2007. 91. 241916. doi:10.1063/1.2825283.
11. X. X. Zhang et al. *Physical Review B*. 2007. 76. 132403. doi: 10.1103/Phys Rev. B.76.132403.
12. D. H. Wang et al. *Journal of Applied Physics*. 2007. 102. 13909. doi:10.1016/j.ssc.2008.02.005.
13. J. Du et al. *Journal of Physics D: Applied Physics*. 2007. 40. 5523. doi:10.1088/0022-3727/40/18/001.
14. M. Khan et al. *Journal of Applied Physics*. 2007. 101. 053919. doi:10.1063/1.2710779.
15. T. Krenke et al. A. Planes. *Physical Review B*. 2005. 72. 014412. doi:10.1103/Phys Rev B.72.014412.
16. P. J. Brown et al. *Journal of Physics*. 2006. 18. 2249. doi:10.1088/0953-8984/18/7/012.
17. K. Koyama et al. *Applied Physics Letters*. 2006. 89. 132505. doi:10.1063/1.2374868.
18. S. Kartha et al. *Physical Review B*. 1995. 52. 803. doi: 10.1103/Phys Rev. B.52.803.
19. S. B. Roy et al. *Phase Transitions*. 2004. 77. 767. doi:10.1103/Phys Rev. B.77.012404.
20. S. Chatterjee et al. *Journal of Physics*. 2007. 19. 346213. doi:10.1088/0953-8984/19/34/346213.
21. J. D. Santos et al. *Journal of Applied Physics*. 2008. 103. 07B326, doi:10.1063/1.2832330.
22. B. Hernando et al. *Applied Physics Letters*. 2008. 92:042504. doi:10.1063/1.2838356.
23. M. Wuttig et al. *Journal of Applied Physics*. 2000. 87. 4707. doi:10.1063/1.3393961.
24. Byung Sang Choi. *IEEE Transactions on Magnetics*. 2006. 42(7). doi: 10.1109/TMAG.2006.874305.

25. R. Colle et al. *Journal of Thermal Analysis and Calorimetry*. 2010. 99. 905–909p. doi 10.1007/s10973-009-0489-2.
26. C. Auguet et al. *Journal of Thermal Analysis and Calorimetry*. 2007. 89. 537–542p.
27. V. Torra et al. *Journal of Thermal Analysis and Calorimetry*.. 2010. 102. 671–680p. doi 10.1007/s10973-009-0613-3.
28. J. Bonastre et al. *Journal of Thermal Analysis and Calorimetry*.. 2007. 88. 83–86p. doi: 10.1007/s10973-006-8092-2.
29. A. Gonzalez et al. *Journal of Thermal Analysis and Calorimetry*. 2007. 87. 255–258p. doi: 10.1007/s10973-006-7802-0.

